Colossal Magnetoresistance in Manganites as a Multicritical Phenomenon

Shuichi Murakami[1] and Naoto Nagaosa[1,2]
[1]*Department of Applied Physics, University of Tokyo, Bunkyo-ku, Tokyo 113-8656, Japan*
[2]*CERC, AIST Tsukuba Central 4, Tsukuba 305-8562, Japan*
(Received 16 August 2002; published 13 May 2003)

The colossal magnetoresistance in manganites $A\mathrm{MnO}_3$ is studied from the viewpoint of multicritical phenomena. To understand the complicated interplay of various phases, we study the Ginzburg-Landau theory in terms of both the mean-field approximation and the renormalization-group analysis for comparison with the observed phase diagram. Several novel features, such as the first-order ferromagnetic transition and the dip in the transition temperature near the multicritical point, can be understood as being driven by enhanced fluctuations near the multicritical point. Furthermore, we obtain a universal scaling relation for the H/M versus M^2 plot (Arrott plot), which fits rather well with the experimental data, providing further evidence for the enhanced fluctuation.

DOI: 10.1103/PhysRevLett.90.197201 PACS numbers: 75.47.Gk, 64.60.Kw, 75.40.Cx, 75.60.Ej

Colossal magnetoresistance (CMR) in manganites is one of the most dramatic phenomena in strongly correlated electronic systems, and extensive experimental studies have revealed many aspects of this effect [1,2]. However, its mechanism has been the subject of long-standing debates; many theories have been proposed such as double exchange [3], polaronic effect [4], and phase separation combined with percolation [5,6] and Griffiths singularity [7]. Shown in Figs. 1 are phase diagrams of the CMR manganites. They clearly evidence that the CMR is related to the concomitant antiferromagnetic (AF) spin ordering, charge ordering (CO), and orbital ordering (OO). Near the phase boundary between the AF/CO/OO and the ferromagnetic metallic (FM) state, the transition temperature has a sharp dip and the critical magnetic field H_c is reduced considerably. Hence, the CMR is collective and differs from single particle properties such as the transition from small to large polarons.

One of the subtle issues is the effect of randomness. The ramdomness induced by alloying or nonuniform strain easily alters critical properties near the phase boundary. Figures 1 show (a) $\mathrm{Pr}_{0.55}$ $(\mathrm{Ca}_{1-y}\mathrm{Sr}_y)_{0.45}\mathrm{MnO}_3$ and (b) $(\mathrm{Nd}_{1-y}\mathrm{Sm}_y)_{0.55}$ $\mathrm{Sr}_{0.45}\mathrm{MnO}_3$. It is not trivial which is more disordered, namely, alloying (a) alkaline-earth atoms or (b) rare-earth atoms. There are, however, three reasons to believe that (a) shows more intrinsic properties than (b) which is dominated by disorder. The first is that strong suppression of the FM transition temperature and appearance of the spin-glass state in (b) is well reproduced by model calculation [6]. The second is that the phase diagrams in ordered and disordered manganites $Ln_{1/2}\mathrm{Ba}_{1/2}\mathrm{MnO}_3$ [10,11] closely resemble Fig. 1(a) and 1(b), respectively. The third is that the scaling fit works almost perfectly in (a), while it does only in the limited region in (b), as shown in this Letter. In (b), the region near the phase boundary is dominated by disorder. An appealing scenario for this is the phase separation and percolation of conducting paths [6]. It assumes a mixture of metallic and insulating domains; the magnetic field expands the metallic domains to result in the CMR. It is a static picture of the resistance network model controlled by the magnetic field. However, diffuse x-ray scattering and Raman scattering experiments revealed that fluctuation is dynamic [1]. Hence, we need to take into account thermal and quantum fluctuations near the phase boundary. It is well known that fluctuation is enhanced near a multicritical point, where more than 2 orders collide. In this Letter we propose a new scenario that the CMR originates from the enhanced fluctuation near the multicritical point, which is controlled by weak magnetic field. We construct the phenomenological Ginzburg-Landau (GL) model by symmetry argument, and give a renormalization-group (RG) analysis for the multicritical phenomena to compare with experiments. This picture explains the scaling law and the first-order ferromagnetic transition as well as the enhanced sensitivity to the magnetic field near the phase boundary.

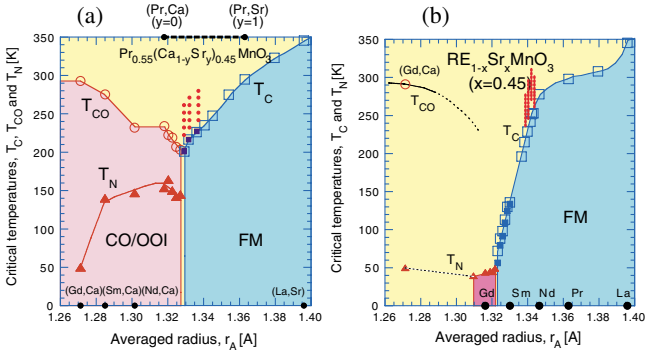

FIG. 1 (color). Phase diagram for (a) $\mathrm{Pr}_{0.55}(\mathrm{Ca}_{1-y}\mathrm{Sr}_y)_{0.45}-\mathrm{MnO}_3$ [8] and (b) $(\mathrm{Nd}_{1-y}\mathrm{Sm}_y)_{0.55}\mathrm{Sr}_{0.45}\mathrm{MnO}_3$ [9]. The averaged radius r_A roughly scales with the bandwidth W. Solid squares represent a first-order transition. Red dots represent the data used in our scaling analysis. The red region at $0\ \mathrm{K} < T < 50\ \mathrm{K}$ in (b) is a spin-glass phase.

The ordering pattern of AF/CO/OO is complicated with an enlarged unit cell. Several microscopic models have been proposed [12]. We employ here instead the GL theory. We classify possible terms in the free-energy functional according to the symmetry of the order parameters. The relevant order parameters are those of ferromagnetism $\vec{M}$, antiferromagnetism $\vec{S}$, charge ordering ρ, and orbital ordering $\vec{T}$. Here, we discuss the dimensionality of each order parameter. Both $\vec{M}$ and $\vec{S}$ are three dimensional, while ρ is scalar. The orbital pseudovector $\vec{T}$ is originally three dimensional but in the presence of the Jahn-Teller interaction, which prefers real linear combinations of the two wave functions $x^2 - y^2$ and $3z^2 - r^2$, it should be regarded as two dimensional: $\vec{T} = (T_x, T_z)$. The free-energy functional should be rotationally invariant in the spin space, but not in the orbital pseudospin space. Hence, $\vec{M}$ and $\vec{S}$ should appear in the form of $\vec{M}^2$ and $\vec{S}^2$. In contrast, third-order terms in $\vec{T}$'s are allowed, because $-\vec{T}$ is not equivalent to $\vec{T}$.

From the spatial pattern of the AF/CO/OO, a wave number of each order parameter is the following, ρ: $(\pi, \pi, 0)$, $\vec{S}$: $(\pi, 0, \pi)$, $(0, \pi, \pi)$, $(\pm\pi/2, \mp\pi/2, \pi)$, $\vec{T}$: $(0, 0, 0)$, $(\pi, \pi, 0)$, $(\pm\pi/2, \pm\pi/2, 0)$, $\vec{M}$: $(0, 0, 0)$. Therefore, the allowed terms in the GL functional are

$$F = \frac{1}{2}\int d^3r \Big[(\nabla\vec{M})^2 + (\nabla\vec{S})^2 + (\nabla\vec{T})^2 + (\nabla\rho)^2 + r_M(\vec{M})^2 + r_S(\vec{S})^2 + r_T(T)^2 + r_\rho(\rho)^2 + g_{\rho S}\rho\vec{S}^2 + (r^x_{\rho T}T_x + r^z_{\rho T}T_z)\rho + g_{\rho M}\rho^2\vec{M}^2 + g_T \mathrm{Re}(T_x + iT_z)^3 + \frac{1}{2}u_M(\vec{M})^4 + \frac{1}{2}u_S(\vec{S})^4 + \frac{1}{2}u_T(\vec{T})^4 + \frac{1}{2}u_\rho\rho^4 \Big]. \tag{1}$$

It is derived by expanding the free energy in terms of the order parameters. The quadratic coefficient r_a ($a = \vec{M}, \vec{S}, \vec{T}, \rho$) is proportional to $1 - U_a\Pi_a(q = 0)$, where U_a is the interaction driving the order a, and $\Pi_a(q)$ is the generalized susceptibility at wave number q. In general, because $\Pi_a(0)$ increases as the temperature T decreases, r_a is an increasing function of T, and is proportional to $T - T_a$ with the mean-field transition temperature T_a. Its dependence on the bandwidth W is less trivial. Itinerancy competes with the CO, OO, and AF orderings, while the FM is induced by the itinerancy itself, i.e., double exchange mechanism. Therefore r_ρ, r_T, and r_S are decreasing functions of W, while r_M has opposite dependence. The terms with derivatives in (1) arise from q^2 terms in the expansion of $\Pi(q)$ in q. By rescaling the order parameters, the coefficients of these terms become $1/2$. Coefficients of higher order terms are put to be constant as in the usual GL theory [13]. The GL approach is based on a small number of essential ingredients such as symmetry and dimensionality of the system, and is independent of microscopic details. It is advantageous in analyzing critical phenomena.

Some remarks are in order. First, the bilinear term between ρ and $\vec{T}$ enforces that the two orders accompany each other, which agrees with experiments. Second, the third-order term in $\vec{T}$ makes the transition first order. However, the magnitude of the jump at the transition depends on the relative values of r_ρ and r_T; if $r_\rho \ll r_T$, it is nearly second order, while it is strongly first order in the other limit. Experimentally, the CO/OO transition is nearly second order, implying that the transition is driven by the CO. Hence, we neglect below the orbital ordering $\vec{T}$. Third, the term $\rho\vec{S}^2$ prohibits the AF *without* the CO; the CO occurs at a temperature higher than or as high as the AF, which agrees with Fig. 1.

Below we are interested in the multicritical phenomenon involving three orders: ρ, $\vec{S}$, and $\vec{M}$. By minimizing the free energy in (1), we obtain three possible mean-field phase diagrams near the multicritical point as shown in Fig. 2. Figure 2(a) is the most relevant to the experiments. Nonetheless, this mean-field analysis cannot capture several experimental features. One is the first-order FM transition in the wide-bandwidth side. Another is the dip of the transition temperatures of FM and CO/OO near the critical bandwidth W_c. These two features are due to the fluctuations enhanced near W_c.

We now turn to the RG analysis of this fluctuation and its effect on the M-H curve. Let us consider a system with competing two order parameters $\vec{M}$ and ρ, with the dimensions $N_M = 3$ and $N_\rho = 1$, respectively. The antiferromagnetic order $\vec{S}$ is neglected because it has the lower transition temperature. From Eq. (1), we pick up terms relevant to these two orders. This is the standard GL functional describing multicritical phenomena, and is studied by the RG analysis in [14]. The fluctuation-induced first-order transition [15] occurs when $g_{\rho M} > \sqrt{u_M u_\rho}$ and $N_M + N_\rho \geq 4$ [16]. To analyze the M-H curve, we use the effective potential [17] including the fluctuation effects. Bare coefficients in the effective potential are renormalized to remove ultraviolet divergence in the one-loop correction, namely, the lowest-order terms in $\epsilon = 4 - d$ [17]. Although we have not studied higher order terms in ϵ, it is known that the lowest-order correction fits well with experiments in usual second-order transitions [17]. By adding counterterms, we get

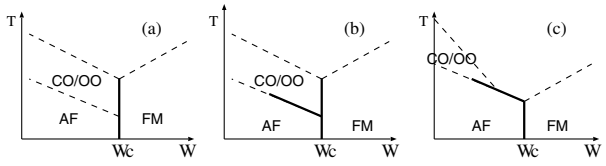

FIG. 2. Mean-field phase diagrams for the GL functional (1). Here W is the bandwidth and T is the temperature. The broken (solid) lines represent the second (first)-order phase transitions.

$$F = \frac{1}{2}(r_M M^2 + r_\rho \rho^2) + \frac{1}{4}(u_M M^4 + 2g_{\rho M} M^2 \rho^2 + u_\rho \rho^4) + (N_M - 1)\frac{\alpha_M^2}{8}\left(\ln\frac{\alpha_M}{\kappa^2} + \frac{1}{2}\right) + \frac{\gamma_+^2}{8}\left(\ln\frac{\gamma_+}{\kappa^2} + \frac{1}{2}\right) + (N_\rho - 1)\frac{\alpha_\rho^2}{8}\left(\ln\frac{\alpha_\rho}{\kappa^2} + \frac{1}{2}\right) + \frac{\gamma_-^2}{8}\left(\ln\frac{\gamma_-}{\kappa^2} + \frac{1}{2}\right), \quad (2)$$

where κ is a parameter setting momentum scale, and

$$\begin{pmatrix}\alpha_M\\ \alpha_\rho\end{pmatrix} = \begin{pmatrix}r_M\\ r_\rho\end{pmatrix} + \begin{pmatrix}u_M & g_{\rho M}\\ g_{\rho M} & u_\rho\end{pmatrix}\begin{pmatrix}M^2\\ \rho^2\end{pmatrix}, \qquad \begin{pmatrix}\beta_M\\ \beta_\rho\end{pmatrix} = \begin{pmatrix}r_M\\ r_\rho\end{pmatrix} + \begin{pmatrix}3u_M & g_{\rho M}\\ g_{\rho M} & 3u_\rho\end{pmatrix}\begin{pmatrix}M^2\\ \rho^2\end{pmatrix},$$
$$\gamma_+ + \gamma_- = \beta_M + \beta_\rho, \quad \gamma_+\gamma_- = \beta_M\beta_\rho - 4g_{\rho M}M^2\rho^2.$$

The quantities r_i, u_i, $g_{\rho M}$ are renormalized.

Because we will analyze the data shown as red dots in Fig. 1, i.e., the wider bandwidth side without the charge order, we set $\rho = 0$. This ρ refers to the expectation value, and its fluctuation is already considered in (2). The fluctuation-induced first-order transition occurs when the RG flow runs into an unstable region of the model. It means that sixth-order terms omitted in (1) are necessary for stability, leading to a first-order transition. Hence, if the RG flow crosses the boundary of the stability region, $u_M = 0$, the system undergoes a first-order transition to the FM phase. Thus, we should follow the RG flow for u_M, u_ρ, $g_{\rho M}$ [14] until $u_M = 0$. Let κ_1 denote the value of κ when $u_M(\kappa) = 0$. Other quantities r_M, r_ρ, M are renormalized multiplicatively, i.e., $r_i(\kappa_1) = r_i h(\kappa_1)$, $M(\kappa_1) = Mg(\kappa_1)$, where r_i and M are the initial values. Thus, renormalization is merely a change of scale for them. The condition $u_M(\kappa_1) = 0$ simplifies the free energy as $F = \frac{1}{2}r_M M^2 + N_M f(r_M) + N_\rho f(r_\rho + g_{\rho M}M^2)$, where $f(x) = \frac{x^2}{8}(\ln x + \frac{1}{2})$ and κ_1 is set as unity by rescaling other variables. The equation of state is

$$H = \frac{\partial F}{\partial M} = r_M M + 2MN_\rho g_{\rho M} f'(r_\rho + g_{\rho M}M^2). \quad (3)$$

It is convenient to rewrite (3) as

$$H/M = r_M + 2g_{\rho M}N_\rho f'(r_\rho + g_{\rho M}M^2). \quad (4)$$

Hence, the (H/M)-M^2 curve, called the Arrott plot, shifts parallel by changing temperature or bandwidth. In a certain range of temperature and bandwidth this curve crosses the horizontal axis. Then some part of the curve becomes unphysical, and the system undergoes a first-order transition by changing the magnetic field. The system is ferromagnetic or metamagnetic.

To verify this scenario, we used two series of data in Figs. 1: (a) for $y = 0.25, 0.3, 0.4$ and (b) for $0.1 \le y \le 0.4$. We can regard y as a parameter controlling the bandwidth. Then r_M and r_ρ are functions of y and T while $g_{\rho M}$ is a constant. We expand r_M and r_ρ near the multicritical point as $r_i = c_{iT}\Delta T + c_{iy}\Delta y$ $(i = M, \rho)$, where $c_{MT}, c_{\rho T}, c_{My}, c_{\rho y}$ are constants. In view of (4), $c_{MT}, c_{\rho T}$ $(c_{My}, c_{\rho y})$ represents an amount of parallel shift of the plot when the temperature T (doping y) changes. We fitted the data as follows. First we varied $c_{MT}, c_{\rho T}, c_{My}, c_{\rho y}$ so that the plots for various y and T overlap most after the parallel shift. Then the abscissa and the ordinate are rescaled to fit to (4). We used the data shown as red dots in Figs. 1. We discarded the data with $M > 1.6\mu_B$, because when the magnetization approaches saturation, the GL functional up to quartic order is no longer appropriate. We also discarded the data for $0.5 \le y \le 0.8$ in (b). They do not fit well with the scaling curve. It is reasonable because in (b) multicritical fluctuations are washed out.

The result is shown in Fig. 3. The plots fall into one curve with good accuracy. This shows that the fluctuation is enhanced near the multicritical point. Because the critical scaling (4) holds for a wide range of data in Fig. 1, the critical region is large (~ 80 K). It manifests strong correlation of electrons in the manganites. Whether the system is critical or not is determined by ξ, measured by a length scale $\xi_0 \sim \frac{E_F}{\Delta}a$, where Δ is a gap, a is a lattice constant, and E_F is the Fermi energy. In the manganites $\Delta \sim 0.5$ eV [18] and $E_F \sim 1$ eV [19] yields $\xi_0 \sim 2a$. Temperature dependence of ξ in a related compound$Pr_{0.5}Ca_{0.5}MnO_3$ can be obtained from Fig. 2(c) of [20]. It is $\xi \sim 100$ Å near the transition temperature $T_c = 235$ K, and is $\xi \sim 20$ Å even at 300 K, which is 65 K higher than T_c. Therefore, ξ is much longer than ξ_0 in the wide temperature range, implying that the critical region is large.

The enhanced fluctuation makes the system sensitive to the magnetic field H. The CO/OO state easily becomes the FM state by a weak magnetic field. Let H_c denote this critical field. An exponent x defined by $H_c \propto (W_c - W)^x$ represents the sensitivity to the external field. Without the fluctuation, x is equal to unity. On the other hand, in the multicritical region but not in the fluctuation-induced first-order-transition region, x is controlled by the bicritical fixed point, and is larger than unity. The $(4 - \epsilon)$ expansion up to $O(\epsilon^2)$ in the isotropic ϕ^4 model results in $x = \frac{\beta\delta}{\phi} \sim 1.37$, where the critical exponents δ, β, and the crossover exponent ϕ are $\delta \sim 4.46$, $\beta \sim 0.39$, $\phi \sim 1.27$ [21]. It can be compared with an experimental value $x \sim 1.6$, from the data for $Pr_{0.65}(Ca_{1-y}Sr_y)_{0.35}MnO_3$ [22]. This increase of x near the multicritical point, i.e., sensitivity to the external field, emerges as the CMR.

Here we discuss the effect of disorder. The bicritical fixed point described above is stable against weak randomness of the coefficients r_M and r_ρ according to Harris criterion [17]. Therefore, our analysis based on the

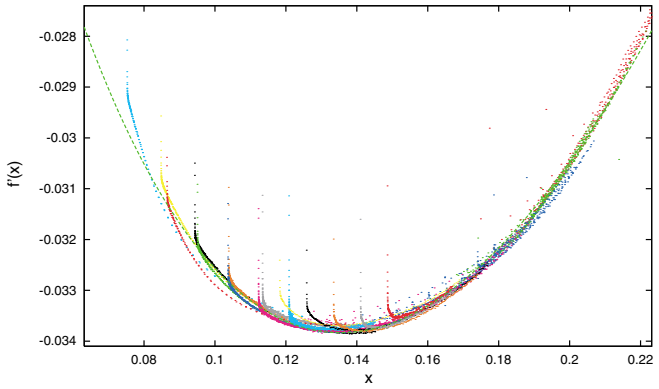

FIG. 3 (color). Scaling plot for (a) $Pr_{0.55}(Ca_{1-y}Sr_y)_{0.45}MnO_3$ and (b) $(Nd_{1-y}Sm_y)_{0.55}Sr_{0.45}MnO_3$. The broken line represents the $f'(x) = \frac{x}{4}(\ln x + 1)$ plot.

bicritical fixed point remains valid for the weak disorder as in Fig. 1(a). In the strong disorder, on the other hand, the first-order transition separating the FM and CO insulating phases is essentially modified by phase separation leading to the sharp drop of the transition temperature as in Fig. 1(b) [6]. The temperature region $T_c < T < T_c^{(0)}$, where $T_c^{(0)}$ is the transition temperature for the pure system while T_c is the suppressed one by random dilution, is characterized as the Griffiths phase [23], and thermodynamic singularites near T_c in the samples with phase separation have been discussed in terms of the Griffiths singularity [7]. This scenario [6,7] leads to the percolation mechanism of CMR, where the resistivity will depend sensitively on random realization of the metallic paths, etc., and consequently on samples. This behavior has been actually observed in dilutely Cr-doped manganites [24]. Cr ions destroy the CO/OO locally, and introduce the FM region. In these dilutely doped samples, the resistivity at low temperature depends on the Cr concentration dramatically, and the hysteresis appears in the temperature cycle. In contrast, when the Cr concentration increases, the resisivity no longer depends on samples or heat cycle. In the latter case, the thermodynamic phases are well defined and the CMR is triggered by the phase change between them, which is the subject of our study here. Hence the present work is complementary to Refs. [6,7]. There are two types of the CMR; one is due to the percolating path and the other is due to the multicritical fluctuation near the phase change. Another interesting issue is the zero temperature Griffiths phase, where the Griffiths singularities influence the whole quantum critical phenomena. In the manganites, this possibility seems to be prevented by the glassy state appearing at low temperatures.

We would like to thank Y. Tokura, Y. Tomioka, E. Dagotto, and H. Kageyama for fruitful discussions. This work is supported by Grant-in-Aids from the Ministry of Education, Culture, Sports, Science, and Technology.

[1] Y. Tokura and N. Nagaosa, Science **288**, 462 (2000), and references therein.
[2] E. Dagotto, T. Hotta, and A. Moreo, Phys. Rep. **344**, 1 (2001).
[3] N. Furukawa, J. Phys. Soc. Jpn. **63**, 3214 (1994).
[4] A. J. Millis, P. B. Littlewood, and B. I. Shraiman, Phys. Rev. Lett. **74**, 5144 (1995).
[5] S. Mori, C. H. Chen, and S-W. Cheong, Phys. Rev. Lett. **81**, 3972 (1998); Y. Moritomo, Phys. Rev. B **60**, 10 374 (1999); M. Uehara *et al.*, Nature (London) **399**, 560 (1999).
[6] A. Moreo, S. Yunoki, and E. Dagotto, Science **283**, 2034 (1999); J. Burgy *et al.*, Phys. Rev. Lett. **87**, 277202 (2001).
[7] M. B. Salamon, P. Lin, and S. H. Chun, Phys. Rev. Lett. **88**, 197203 (2002).
[8] Y. Tomioka and Y. Tokura, Phys. Rev. B **66**, 104416 (2002).
[9] Y. Tomioka and Y. Tokura (to be published).
[10] D. Akahoshi *et al.*, Phys. Rev. Lett. **90**, 177203 (2003).
[11] H. Kageyama *et al.*, cond-mat/0208518; T. Nakajima *et al.*, cond-mat/0207410.
[12] J. van den Brink, G. Khaliullin, and D. Khomskii, Phys. Rev. Lett. **83**, 5118 (1999); I. V. Solovyev and K. Terakura, Phys. Rev. Lett. **83**, 2825 (1999).
[13] L. D. Landau and E. M. Lifshitz, *Statistical Physics* (Pergamon Press, Oxford, 1980), Chap. XIV.
[14] D. R. Nelson, J. M. Kosterlitz, and M. E. Fisher, Phys. Rev. Lett. **33**, 813 (1974); J. M. Kosterlitz, D. R. Nelson, and M. E. Fisher, Phys. Rev. B **13**, 412 (1976).
[15] D. J. Wallace, J. Phys. C **6**, 1390 (1973); T. Natterman and S. Trimper, J. Phys. A **8**, 2000 (1975); S. A. Brazovskii and I. E. Dzyaloshinskii, JETP Lett. **21**, 164 (1975); J. Rudnick, Phys. Rev. B **18**, 1406 (1978); E. Domany, D. Mukamel, and M. E. Fisher, Phys. Rev. B **15**, 5432 (1977).
[16] S. Murakami and N. Nagaosa, J. Phys. Soc. Jpn. **69**, 2395 (2000).
[17] D. J. Amit, *Field Theory, the Renormalization Group and Critical Phenomena* (World Scientific, Singapore, 1993), and references therein; H. H. Iacobson and D. J. Amit, Ann. Phys. (N.Y.) **133**, 57 (1981).
[18] Y. Okimoto *et al.*, Phys. Rev. B **59**, 7401 (1999).
[19] R. Maezono, S. Ishihara, and N. Nagaosa, Phys. Rev. B **58**, 11583 (1998).
[20] S. Shimomura *et al.*, Phys. Rev. B **62**, 3875 (2000).
[21] M. E. Fisher, Rev. Mod. Phys. **46**, 597 (1974).
[22] Y. Tomioka *et al.*, J. Phys. Soc. Jpn. **66**, 302 (1997).
[23] R. B. Griffiths, Phys. Rev. Lett. **23**, 17 (1969).
[24] B. Raveau, A. Maignan, and C. Martin, J. Solid State Chem. **130**, 162 (1997); T. Kimura *et al.*, Phys. Rev. Lett. **83**, 3940 (1999).